

Experimental Oscillation Death in Two Mutually Coupled Light-Controlled Oscillators

Gabriela Conde-Saavedra^{1, a)} and Gonzalo Marcelo Ramírez-Ávila^{1, b)}

*Instituto de Investigaciones Físicas, Universidad Mayor de San Andrés,
Casilla 8635. La Paz, Bolivia*

We characterized the synchronous behavior of two mutually coupled light-controlled oscillators to determine their relevant parameters that allow validation of our model that predicts oscillation death for strong coupling. We experimentally verified the predictions mentioned above and identified the critical coupling (distance) for which oscillation death starts to manifest itself.

PACS numbers: 0.5.45.Xt, 84.30.Ng, 85.60.Jb, 43.75.+a, 05.45.Tp, 05.45.Jn

Keywords: Synchronization; coupled oscillators; Oscillators, pulse generators, and function generators; Light-emitting devices.

^{a)}gazzurra@gmail.com

^{b)}gramirez@ulb.ac.be

While the characterization of the synchronous behavior of a system of two mutually coupled light-controlled oscillators has been extensively studied, few studies were done when coupling strength takes high values and none for the case in which a strong coupling enables the transition to an oscillation death regime. We used a model for light-controlled oscillators to establish the synchronization conditions and also the situation in which a tendency to produce oscillation quenching is due to a strong coupling between these oscillators. According to the model, there is a critical value for which oscillation death appears, and above this one, oscillation death is manifested with distinctive features. We experimentally verified the model predictions concerning the transition from synchronization to oscillation death as the coupling strength increases. Experimental results on oscillation death are scarce in relaxation oscillators, and our research constitutes a detailed report of the experimental oscillation death on pulse-coupled oscillators.

I. INTRODUCTION

Synchronization is a common phenomenon in which two or more oscillators adjust their rhythms due to a coupling mechanism. The first observation of this was made by C. Huygens (1665) on two independent pendulum-clocks hanging on the wall of his room, achieving anti-phase synchronous oscillations eventually. Even though the system of Huygens' pendulum clocks was considered as a paradigmatic example of synchronization, the mechanisms, and features of this phenomenon were recently unveiled in several works where the authors revisited this system¹⁻³. Further studies of synchronization on two pendulum clocks were done finding interesting aspects such as the possibility of in-phase oscillation⁴, clustering synchronization^{5,6} and several improvements on this kind of systems for a better understanding of synchronization⁷. Under the same perspectives, studies on synchronization of metronomes were done by Bennett *et al.*¹, Czolczynski *et al.*², Pantaleone⁸, and Hoogeboom *et al.*⁹ finding both phase and anti-phase modes of synchronization. Although Huygens' experimental and mathematical model might be considered the formal founding work on synchronization; other models were used to study synchronization in a variety of systems such as sinus node cells^{10,11}, neural networks¹², animal gaits¹³, fireflies¹⁴⁻¹⁶, rhythmic applause¹⁷, circadian cycles¹⁸ among others.

A particularly astonishing synchronization phenomenon is seen in groups of fireflies when at

the beginning of their gatherings, each one flashes independently with its own frequency, then starts influencing others optically and finally, all adjust their frequencies achieving a unison lighting show. Even though synchronized flashing of fireflies had been already reported in the XVII century by Dutch physician E. Kaemper¹⁹, it has been in recent years that scientists modelled the phenomena in a theoretical and experimental way^{14,20–22} leading to interesting results. Based on the electronic system built by Ramírez-Ávila *et al.*²³, firefly behavior has been mimicked by arranges of LM555 based-oscillators, where Rubido *et al.*²⁴ have studied the coupling through light pulses under different modes of interactions such as mutual and master-slave.

Another emergent phenomenon is oscillation suppression, being reported first by Lord Rayleigh in 1877. He observed two organ pipes with slightly different frequencies, that when placed close to each other, achieved an almost silent state.²⁵ Even since then, this state was known as an oscillation death and has been studied in different human-made and natural coupled oscillating systems such as when the flames of three close candles pass through various modes of synchronization and finally achieve stable combustion interpreted as a death state²⁶. Lately, Koseska *et al.*²⁷ performed a rigorous study of oscillation quenching, setting strict differences between oscillation death (OD) and amplitude death (AD). They also mentioned possible applications of oscillation quenching on pathological cases of neuronal disorder (Alzheimer and Parkinson), or the interaction of insulin-producing cells and diabetes, or the heart cells to regulate cardiac problems. Further essential appliances can also be found in the generation of control mechanisms for lasers.

The purpose of our work is to obtain a better understanding regarding the complete synchronization of mutually coupled fireflies and the arising of OD with increasing coupling strength. We used 555-IC based-oscillators in the form of two mutually coupled light-controlled oscillators (LCOs) with the aim of characterizing their OD regime and comparing the experimental results with those obtained by our model.

A remarkable phenomenon related to the OD has been reported by people who live in the Northern region of Bolivia. They affirm that fireflies caught in a glass jar display synchronous behavior by flashing in unison, then keep their lights on with time intervals so revealing that this glass jar could serve as a portable lamp. The latter behavior in technical terms, tell us that fireflies synchronize because of their mutual interaction followed by an OD regime perhaps due to their proximity and consequently to strong coupling. Our work could feasibly explain this phenomenon.

The article is organized as follows: in Section II are given the formal definitions of synchronization and OD relevant to the work. Section III contains the model used for LCOs. The description of

the experimental setup is shown in Section IV. The data analysis and results are done in Section V. Finally, in Section VI we give the conclusions and perspectives.

II. SYNCHRONIZATION AND OSCILLATION DEATH

In this Section, we describe the general aspects that allow recognizing mathematically and experimentally the presence of both phenomena: synchronization and OD.

A. Synchronization

Synchronization is a relation between phases or frequencies for two or more oscillators²⁸. This is defined as the *phase-locking* regime which is represented by

$$|n\phi_1 - m\phi_2| \leq \text{cte}, \quad n, m \in \mathbb{Z}^+. \quad (1)$$

In our case (LCOs), Eq. (1) is constrained by a constant, where n is the number of pulses of one oscillator and m the number of pulses emitted by the other oscillator. If simultaneous flashes are to be considered between two LCOs then $n = m = 1$. Therefore the condition to determine whether there is or not synchronization in two mutually coupled LCOs (unitary winding number) is $|\Delta\phi| \leq \text{cte}$.

Experimentally, two oscillators are synchronized when stable signals exhibit the phase-locking. The latter allows the measurement of the frequency difference $\Delta\phi$, the synchronization period T_s and its distance d .

According to Rubido *et al.*²², it has been established that for two coupled LCOs the *phase-locking* must be equal or less than the discharging time after coupling t_γ of any of the two oscillators: $|\Delta\phi| \leq t_\gamma$.

B. Oscillation death

With the aim of describing OD for a system of N coupled oscillators, it is possible to use the following set of equations^{27,29}:

$$\frac{dx_i^j}{dt} = F(x_i^j, k) + d_i^j \sum_{j=1}^N (x_i^j - x_i^{j-1}), \quad (2)$$

where $i = 1, \dots, m$ and $j = 1, \dots, N$, m is the dimension, x_i is the phase variable, F is a non-linear function depending on the variable and k parameters, and d_i^j denotes the local coupling mechanism.

If the oscillators are identical, some periodic solutions will appear depending on the type and the strength of the coupling parameter. The d_i^j coupling also gives rise to a combination of steady states and limit cycles. Under particular conditions, the phase space can show one or different values of the phase variables x_i^j corresponding to a homogeneous and an inhomogeneous steady state (HSS and IHSS).

The HSS and the IHSS characterize the AD and the OD phenomena, respectively²⁷. Another difference between these two phenomena lies in the fact that AD exhibits zero amplitude while OD displays zero frequency.

III. THE MODEL

A. Synchronization

We use the LCOs' model developed in Ramírez-Ávila *et al.*²³. Two stages are considered: fired LCO and extinguished LCO. Therefore, there is a binary variable $\epsilon(t)$ for which:

$$\epsilon(t) = \begin{cases} 1, & \text{charging stage or extinguished,} \\ 0, & \text{discharging stage or fired.} \end{cases}$$

The charging and discharging stages in the capacitor are respectively described through the following equations:

$$\frac{dV}{dt} = \lambda(V_M - V), \quad \frac{dV}{dt} = -\gamma V. \quad (3)$$

where time constants related to the shortest intervals (discharging) and longest (charging) are given by:

$$\frac{1}{\lambda} = (R_\lambda + R_\gamma)C, \quad \frac{1}{\gamma} = R_\gamma C. \quad (4)$$

The natural stages of any oscillator, say i , in a situation where there are no other light sources influencing the oscillator, are described as follows:

$$\begin{aligned} \frac{dV_i(t)}{dt} &= \lambda_i(V_{Mi} - V_i(t))\epsilon_i(t), & \frac{V_{Mi}}{3} \leq V_i(t) \leq \frac{2V_{Mi}}{3}, & \epsilon_i(t) = 1, \\ \frac{dV_i(t)}{dt} &= -\gamma_i V_i(t)(1 - \epsilon_i(t)), & \frac{2V_{Mi}}{3} > V_i(t) > \frac{V_{Mi}}{3}, & \epsilon_i(t) = 0. \end{aligned} \quad (5)$$

The transition through the two stages are expressed by the conditions:

$$\begin{aligned} \text{If } V_i(t) = \frac{V_{Mi}}{3} \text{ and } \epsilon_i(t) = 0, \text{ then } \epsilon_i(t_+) = 1, \\ \text{If } V_i(t) = \frac{2V_{Mi}}{3} \text{ and } \epsilon_i(t) = 1, \text{ then } \epsilon_i(t_+) = 0. \end{aligned} \quad (6)$$

For instance, if two LCOs are coupled, then the LCO₁ period is modified by the LCO₂ light pulses, and vice-versa.

B. Oscillation death

Using the model mentioned above and carrying out experiments for diverse distances between the LCOs, we obtained that coupling strength β follows a power-law function with the distance, in the form:

$$\beta = Ad^{-n}, \quad (7)$$

being A a constant.

Note that coupling strength is related to the light intensity of the LEDs, diminishing approximately with the square of the distance. In Sect. [V A](#) are shown the details of how the power n has been obtained.

Considering two coupled LCOs again, the coupling strength, β_{12} modifies the LCO₁ dynamic variable V_1 ; and reciprocally β_{21} modifies V_2 . The resulting equations are:

$$\frac{dV_1(t)}{dt} = \lambda_1(V_{M1} - V_1(t))\epsilon_1(t) - \gamma_1 V_1(t)[1 - \epsilon_1(t)] + \beta_{12}[1 - \epsilon_2(t)], \quad (8)$$

$$\frac{dV_2(t)}{dt} = \lambda_2(V_{M2} - V_2(t))\epsilon_2(t) - \gamma_2 V_2(t)[1 - \epsilon_2(t)] + \beta_{21}[1 - \epsilon_1(t)]. \quad (9)$$

Where we consider a symmetric coupling, *i.e.* $\beta_{12} = \beta_{21}$. The integration of Eqs. (8) and (9) allows us to determine the LCOs synchronization period and the phase difference between them, as well as the graphs for the voltages when the LCOs interact with each other.

IV. EXPERIMENTAL SETUP

A. Synchronization

We built two LCOs, which were aligned over the same base that had a 120.0 cm ruler facilitating the measurement of the distance between the LCOs (See Fig. 1). The oscillators operated with a NE555 integrated circuit, LD242-3 IR LEDs, a 100 k Ω and a 2 k Ω potentiometer that controls respectively the charging and discharging stages. Also, a $C_1 = 0.47 \mu\text{F}$ and a $C_2 = 47 \mu\text{F}$ capacitors (See Fig. 2).

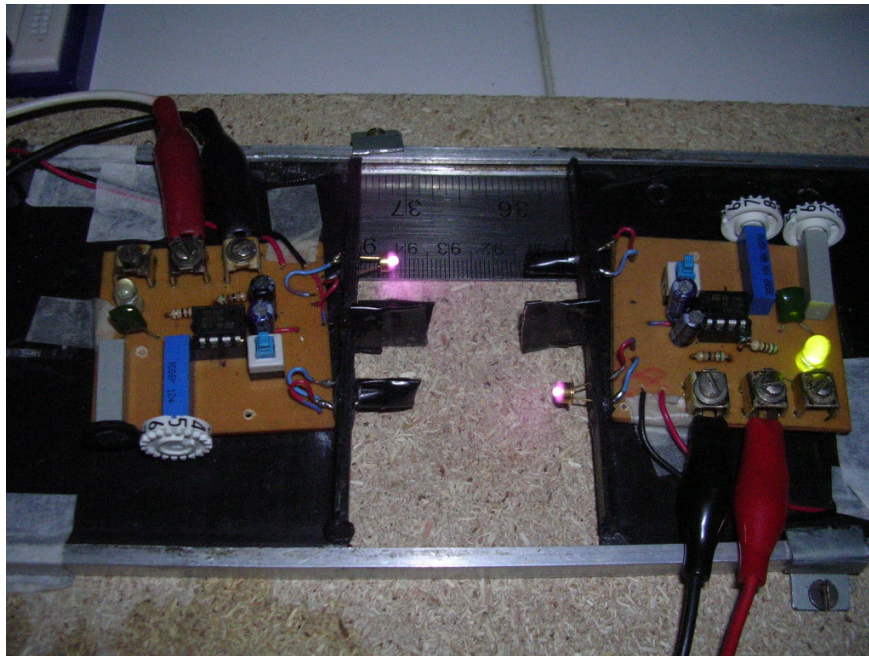


FIG. 1. (Color online) View of the experimental setup showing the LCOs. A base with a ruler on it to measure the distance between the LCOs. When IR-LEDs are covered, LCOs are uncoupled.

Each LCO is connected to a digital oscilloscope through the 0.47 μF capacitor. On the other hand, the connection to the 47 μF capacitor allows to observe the firefly mode of the LCO consisting in the oscillatory flash emission with frequencies corresponding to real fireflies and unaided eye detectable. All diodes are in-series connected to 52.2 Ω fixed resistors in order to avoid burn out. We also used 9 V rechargeable batteries as voltage source.

The *natural period* T of an LCO is the complete period of oscillation when it is uncoupled. Natural periods were adjusted for both LCOs through the potentiometers, to the same value $T_1 = T_2 = (20.00 \pm 0.02)$ ms, constituting the initial situation. In order to simplify measure-

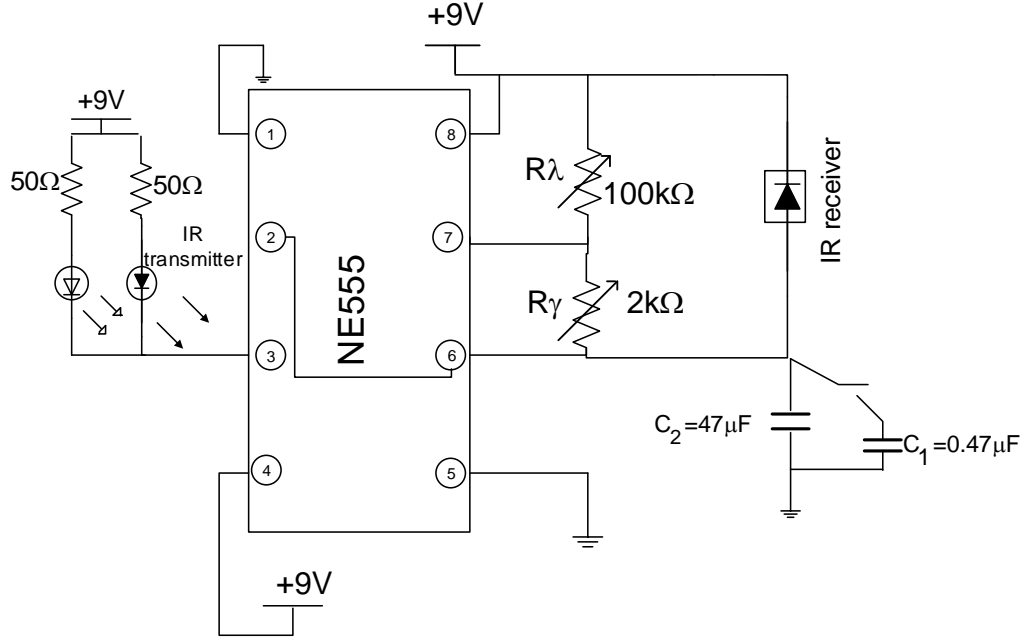


FIG. 2. Oscillator diagram.

ments, we set the discharging time to a constant value, namely: $t_\gamma = (600 \pm 1) \mu\text{s}$. Thus, only the charging time t_λ was regulated by the potentiometer.

One of the LCOs was chosen to be the reference, denoted as LCO_1 , whose natural period was kept constant throughout the experiment. Whereas LCO_2 was fixed on the right extreme of the base setting its natural period before coupling to LCO_1 . Then we varied the mutual distance between the LCOs. Once coupled LCOs achieved the same period, we denoted that as the *synchronization period* T_s . In this context, the following data was registered:

- Distance d ,
- Synchronization period T_s ,
- Discharging times of each LCO: $t_{1\gamma}, t_{2\gamma}$,
- Charging times of each LCO: $t_{1\lambda}, t_{2\lambda}$,
- The phase difference $\Delta\phi$.

The considered distances went from 37.0 cm (maximum possible distance for synchronization according to our experimental measurements for two LCOs with identical natural period of 20.0

cm, as shown in Table I) until a critical distance where OD started its manifestation. For each distance, the charging time of the LCO_2 was varied in order to find the maximum and minimum values that followed the phase-locking condition.

Concerning the coupling mechanisms, it is noteworthy to mention that the pulses of light emitted and received by each LCO are responsible for the coupling, and indeed, the coupling strength is directly proportional to the intensity of light and approximately to the inverse of the square of the distance between LCOs.

B. Oscillation death

The main experimental parameter to characterize OD in two coupled LCOs is their mutual distance. We determined the maximum distance at which LCOs are still able to synchronize. From a distance of 35.0 cm (close to the above mentioned maximum one), we proceeded to approach the LCOs in steps of 5.0 cm until a mutual distance of 5.0 cm. The OD occurs at a distance where the LCOs' oscillatory feature is lost, *i.e.* when they visually remain aglow.

Similarly, the coupled LCOs model allowed us to determine the coupling strength β using Eq. (7) and verifying for an adequate approximation to the oscillation period T_s and the phase difference $\Delta\phi$ of the experimental data. This procedure was done for each distance. Therefore, we obtained both the distance and coupling strength values.

V. ANALYSIS

A. Synchronization

Table I shows the experimental measurements for a setup of two mutually coupled LCOs. The synchronization region was built with the values of $T_{2\min}$, $T_{2\max}$, their error bars and d as depicted in Fig. 3.

We observe that the range of synchronization widens with the decreasing of the mutual distance. The synchronization region is extended in a wide range showing us interaction of the LCOs is also considerable because it goes from 5.0 cm to 37.0 cm. At this latter distance, the system shows the phase-locking condition only if they oscillate basically with the same frequency. For longer distances, the interaction is not strong enough for the achievement of synchronization. For distances shorter than 5.0 cm, phase-locking is still manifested until a critical value of (3.1 ± 0.1) cm.

The model captures the synchronizing characteristics of the phase-locking stage seen similarly in the oscilloscope (Fig. 4). The phase difference is measured in terms of a time interval. We consider synchronous LCOs as long as the time interval related to the phase difference can be measurable.

d [cm]	5.0	10.0	15.0	20.0	25.0	30.0	35.0	37.0
$T_{2\min}$ [ms]	13.12±0.40	18.04±0.15	19.21±0.16	19.64±0.04	19.80±0.04	19.90±0.02	19.94±0.01	
T_s [ms]	9.97±0.63	16.33±0.20	18.44±0.14	19.20±0.05	19.53±0.02	19.70±0.04	19.83±0.02	
$\Delta\phi$ [μ s]	504 ± 17	585 ± 23	587 ± 9	591 ± 6	592 ± 11	563 ± 58	557 ± 55	
T_2 [ms]	20.00	20.00	20.00	20.00	20.00	20.00	20.00	20.00
T_s [ms]	20.16±0.17	20.02±0.10	19.84±0.06	19.81±0.09	19.83±0.08	19.88±0.02	19.88±0.05	19.89±0.04
$\Delta\phi$ [μ s]	42 ± 3	52 ± 14	161 ± 31	268 ± 76	362 ± 94	394 ± 48	500 ± 51	516 ± 56
$T_{2\max}$ [ms]	30.11±0.44	20.97±0.13	20.27±0.12	20.09±0.11	20.08±0.02	20.05±0.01	20.03±0.01	
T_s [ms]	16.97±0.68	17.79±0.27	19.04±0.14	19.94±0.08	20.03±0.14	19.94±0.05	19.92±0.03	
$\Delta\phi$ [μ s]	-461 ± 16	-575 ± 63	-573 ± 49	174 ± 70	221 ± 16	308 ± 29	420 ± 58	

TABLE I. Experimental measurements for a setup of two mutually coupled LCOs.

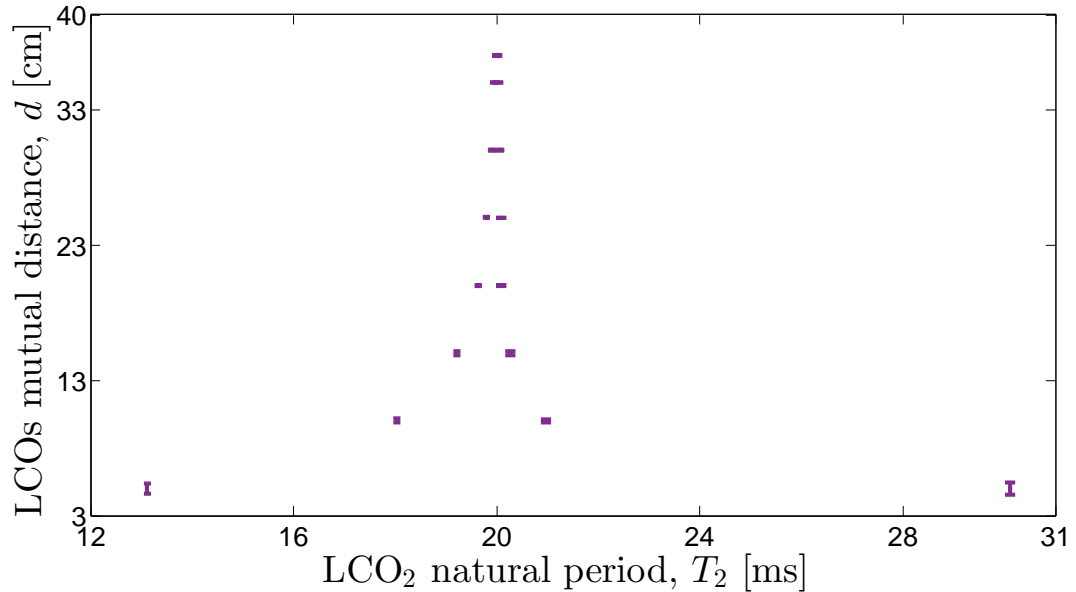


FIG. 3. Synchronization range for LCO₂ when the reference LCO₁ has a natural period of $T_1 = (20.00 \pm 0.02)$ ms.

To simplify operations, the values of resistors for LCO₁ were kept constant, as well as the

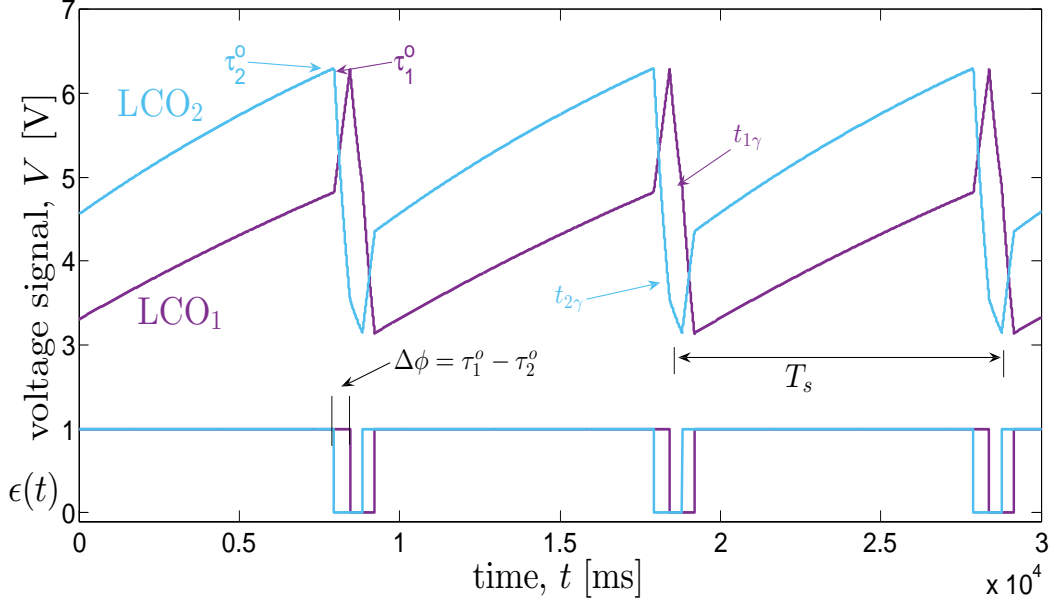


FIG. 4. Phase-locking regime for a setup of two mutually coupled LCOs.

LCO₂'s resistor related to the discharge. Thus, the only variables were R_{γ_2} and β . We consider symmetric coupling.

The synchronization region is determined by the model in terms of the coupling strength and the LCO₂ oscillation period (See Fig. 5).

B. Oscillation death

Experimentally, the oscillation quenching in both mutually coupled LCOs occurred at a distance of (3.1 ± 0.1) cm. In this situation, the LCOs remained lit up, and the oscilloscope showed one voltage steady value.

In order to describe OD, we use Eqs. (8) and (9). Using the charging and discharging times measured for each oscillator we might calculate the values of the resistors R_λ and R_γ by means of Eqs. (4). Initial values of voltages were chosen as: $V_{01} = 5.50$ V, $V_{02} = 3.10$ V; as well as initial values for each oscillator: $\epsilon_{01} = \epsilon_{02} = 1$, showing that both are at the charging stage. According to the experimental values, we consider the source voltages: $V_{1M} = 9.43$ V and $V_{2M} = 9.45$ V.

The appropriate coupling strength and distance values are summarized in Table II. These data are fitted by a power-law (see Eq. (7)), finding the values: $A = (64910 \pm 22760)$ V \cdot s⁻¹ \cdot cm⁻ⁿ

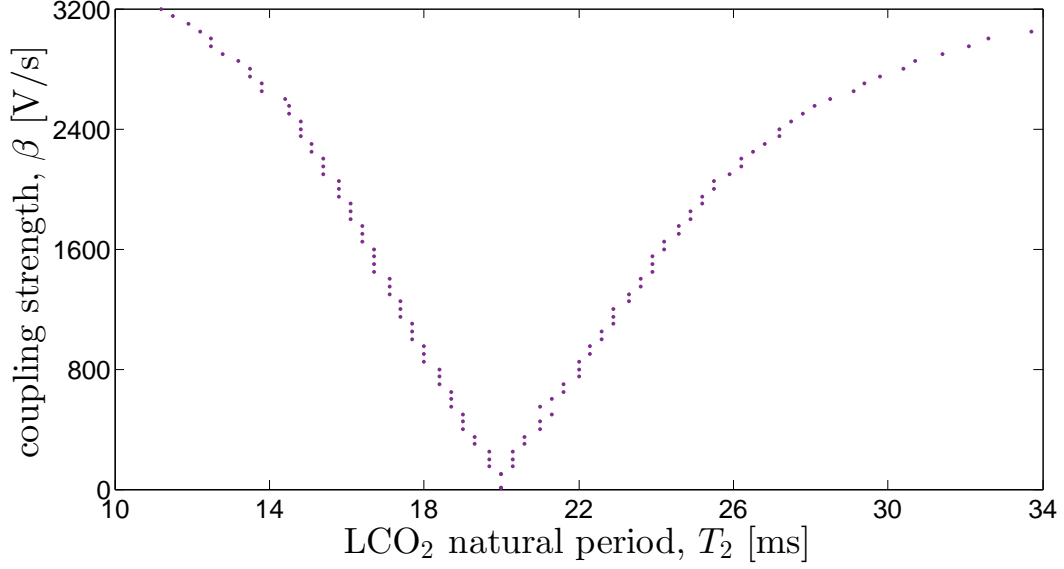


FIG. 5. Synchronization region (Arnold tongue) represented into the plane (T_2, β) .

and $n = -1.95 \pm 0.20$, with a correlation coefficient of $r^2 = 0.9996$.

Thus, the coupling strength as a function of the distance is given by

$$\beta = 64910 \cdot d^{-1.95}. \quad (10)$$

In order to study OD, we use Eq. (10). Taking into account the experimental distance where OD is manifested, $d_{\text{OD-exp}} = (3.1 \pm 0.1)$ cm, we compute the coupling strength value $\beta = (7148 \pm 448)$ V/s. The error interval for the coupling strength is computed with Eqs. (11) and (12) giving, as a result, $[3701, 12243]$ V/s. With these values, using Eqs. (8) and (9), we obtain the waveforms shown in Fig. 6 where we observe the transition from synchronization ($\beta = 2817$ V/s) to OD ($\beta = 5000$ V/s) passing by an anti-synchronous regime shown in (c) and (d); being $T_1 = 13.10$ ms and $T_2 = 20.00$ ms.

On the other hand, with the model we found that OD starts at a coupling strength value $\beta = 5076$ V/s and using Eq. (7) we found the corresponding distance $d_{\text{OD-model}} = 3.7$ cm. The interval values for this coupling strength is $[2530, 8999]$ V/s.

Experimentally, we observed that at a distance of 3.7 cm, the LCOs' waveforms exhibited some instabilities in their oscillations. The latter is because the LCOs are entering to the OD regime.

In Fig. 7 are represented the coupling strength interval values for different distances, where we have considered the relations:

d [cm]	T_s [ms]	$\Delta\phi$ [μ s]	$T_{1\gamma}$ [μ s]	$T_{2\gamma}$ [μ s]	β [V/s]	T_s [ms]	$\Delta\phi$ [μ s]
3.1	-	-	-	-	5076	-	-
5	20.16 ± 0.17	42 ± 3	1386 ± 40	1366 ± 52	2817	20.79	4
10	20.02 ± 0.10	52 ± 14	718 ± 5	700 ± 5	831	20.05	10
15	19.84 ± 0.06	161 ± 31	642 ± 7	633 ± 2	319	19.98	23
20	19.81 ± 0.09	268 ± 76	620 ± 3	615 ± 4	137	19.96	55
25	19.83 ± 0.08	362 ± 94	613 ± 4	609 ± 2	74	19.95	98
30	19.88 ± 0.02	394 ± 48	610 ± 1	606 ± 1	35	19.95	234
35	19.88 ± 0.05	500 ± 51	609 ± 1	603 ± 1	19	19.96	290
37	19.89 ± 0.04	516 ± 56	608 ± 2	603 ± 2	9.2	19.96	488

TABLE II. Left: Experimental results of mutually coupled LCOs with the same natural period. Note that OD is manifested for strong coupling (short distances). Right: Numerical results of the phase difference and the synchronization period when the coupling strength parameter increases until reaching OD.

$$\beta_{\min} = 42150 \cdot d^{-2.15} . \quad (11)$$

$$\beta_{\max} = 87670 \cdot d^{-1.174} . \quad (12)$$

VI. CONCLUSIONS AND PERSPECTIVES

We characterized synchronization region for two mutually coupled LCOs numerically and experimentally. As expected, we observed that the synchronization regions widen as the distance between the oscillators gets smaller. The latter is featured by an almost inverse of the square-distance law whose explicit form is $\beta = A \cdot d^n$, being $A = (64910 \pm 22760) \text{ V} \cdot \text{s}^{-1} \cdot \text{cm}^{-n}$ and $n = -1.95 \pm 0.20$; where these values were obtained by a curve-fitting analysis with a correlation coefficient of $r^2 = 0.9996$. The similar values of the experimental and numerical quenching distance (3.1 ± 0.1) cm and 3.7 cm, respectively, indicate enough concordance that validates the used LCO's model for the OD. Moreover, looking at the error bars whose values are overlapped meaning that the model fits the experimental data and describes the OD behavior appropriately.

The main issue of this work lies in the fact that the LCOs model predicts OD for strong coupling that we corroborated experimentally, and as far as we know, it is the first time that experimental OD in this type of pulse-coupled oscillators is reported. The observed OD implies that the LCOs

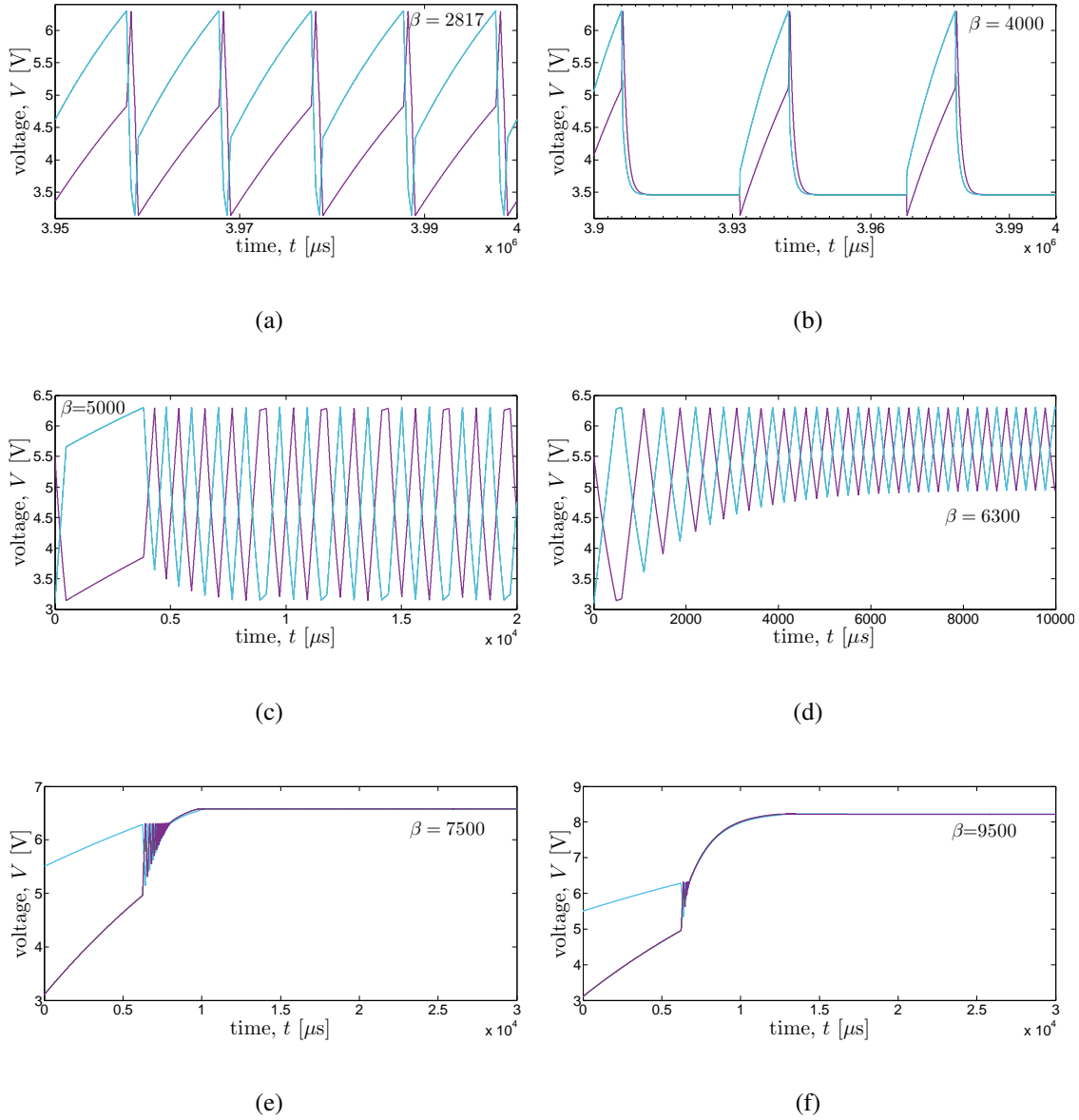


FIG. 6. Transition from synchronization to OD for two interacting LCOs. **(a)** shows the synchronization regime, **(b)** as the coupling strength increases, the system starts leaving the synchronized regime, **(c)** at higher coupling strengths, the synchronized regime turns to an anti-synchronous one, **(d)** frequency of both LCOs increases but amplitude decreases to a range of 1.5 V, **(e)** shows the signals tending to stabilize to a value of 6.7 V and **(f)** shows that at even higher coupling strength the system stabilization tends to 8.2 V.

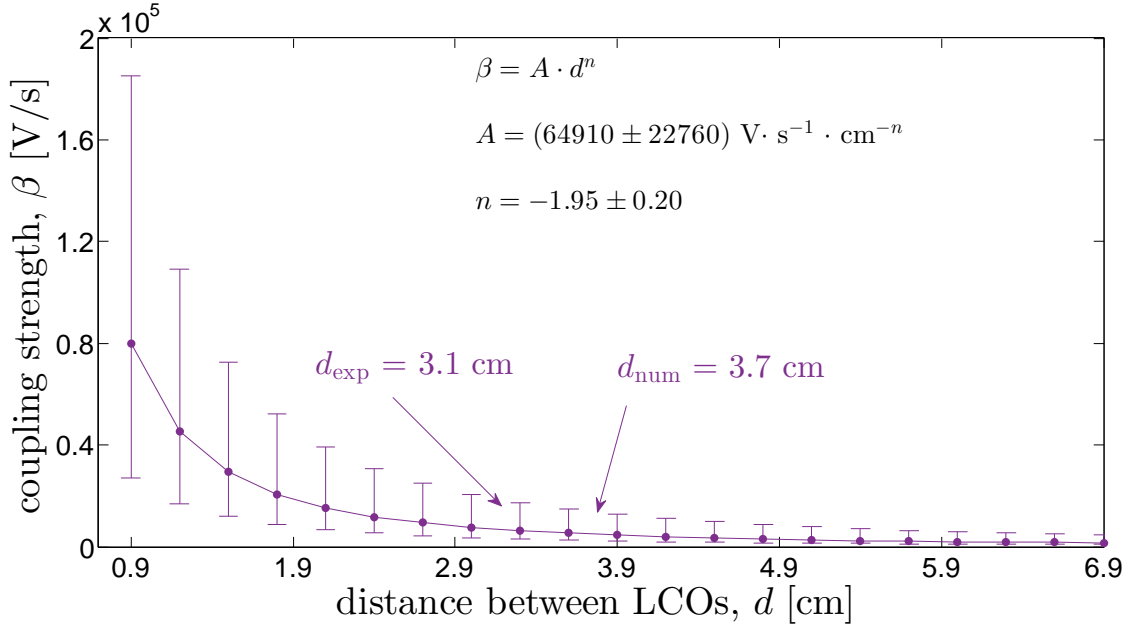


FIG. 7. Coupling strength interval values for different distances. We point out the experimental and numerical distance values where OD is manifested ($d_{\text{exp}} = 3.1 \text{ cm}$ and $d_{\text{num}} = 3.7 \text{ cm}$).

remain permanently lit due to the strong coupling resulting in short distances between the oscillators. The main issue of this work lies in the fact that the LCOs model predicts OD for strong coupling that we corroborated experimentally, and as far as we know, it is the first time that experimental OD in this type of pulse-coupled oscillators is reported. The observed OD implies that the LCOs remain permanently lit due to the strong coupling resulting in short distances between the oscillators. Our results explain or show the claim that a glass jar containing fireflies could be used as lantern because they all remain illuminated for a short time but significantly longer than their natural flash periods. The latter is explained by the fact that the fireflies gathered inside a glass jar could undergo a strong coupling and, therefore, remain illuminated until their fuel is entirely exhausted. In the case mentioned above, this behavior could be related to an OD of the system, and it would be interesting to test experimentally with real fireflies and compare it with the OD between the LCOs that we found in this work.

We expect to characterize the OD transition by means of an exhaustive variation of the coupling strength. We also plan to extend our OD studies for the case of LCOs ensembles in different network configurations.

ACKNOWLEDGMENTS

We acknowledge the help of IIF-UMSA staff that facilitated our work, and we also appreciate the technical advice of Pedro Miranda-Loza, during the experimental work.

REFERENCES

- ¹M. Bennett, M. F. Schatz, H. Rockwood, and K. Wiesenfeld, “Huygen’s clocks,” *Proc. R. Soc. Lond.* **458**, 563–5797 (2002).
- ²K. Czolczynski, P. Perlikowski, A. Stefanski, and T. Kapitaniak, “Huygens’ odd sympathy experiment revisited,” *Int. J. Bifurcat. Chaos.* **21**, 2047–2056 (2011).
- ³K. Wiesenfeld, and D. Borrero-Echeverry, “Huygens (and others) revisited,” *Chaos* **21**, 047515 (2011).
- ⁴R. Dilao, “Antiphase and in-phase synchronization of nonlinear oscillators: The Huygens’s clocks system,” *Chaos* **19**, 023118 (2009).
- ⁵K. Czolczynski, P. Perlikowski, A. Stefanski, and T. Kapitaniak, “Clustering and synchronization of n Huygens’ clocks,” *Physica A* **388**, 5013–5023 (2009).
- ⁶K. Czolczynski, P. Perlikowski, A. Stefanski, and T. Kapitaniak, “Clustering of Huygens’ clocks,” *Prog. Theor. Phys.* **122**, 1027–1033 (2009).
- ⁷J. Peña Ramirez, R.H.B. Fey, K. Aihara, and H. Nijmeijer, “An improved model for the classical Huygens’ experiment on synchronization of pendulum clocks,” *J. Sound Vib.*, **333**, 7248–7266 (2014).
- ⁸J. Pantaleone, “Synchronization of metronomes,” *Am. J. Phys.*, **70**, 992 (2002).
- ⁹F. N. Hoogeboom, A. Y. Pogromsky, and H. Nijmeijer, “Huygens’ inspired multi-pendulum setups: Experiments and stability analysis,” *Chaos*, **26**, 116304 (2016).
- ¹⁰J. Jalife, “Mutual entrainment and electrical coupling as mechanisms for synchronous firing of rabbit sino-atrial pace-maker cells,” *J. Physiol.*, **356**, 221–243 (1984).
- ¹¹D. C. Michaels, E. P. Matyas, and J. Jalife, “Mechanisms of sinoatrial pacemaker synchronization: A new hypothesis,” *Circ. Res.*, **61**, 704–714 (1987).
- ¹²H. D. I. Abarbanel, M. I. Rabinovich, A. Selverston, M. V. Bazhenov, R. Huerta, M. M. Sushchik, and L. L. Rubchinskii, “Synchronization in neural networks,” *Phys-Usp+*, **39**, 337–362 (1996).
- ¹³J. J. Collins, and N. Stewart, “Coupled nonlinear oscillators and the symmetries of animal gaits,”

- J. Nonlinear Sci. , **3**, 349–392 (1993).
- ¹⁴G. B. Ermentrout, “An adaptive model for synchrony in the firefly *Pteroptyx malaccae*,” J. Math. Biol., **29**, 571–585 (1991).
- ¹⁵G. M. Ramírez-Ávila, J.-L. Deneubourg, J.-L. Guisset, N. Wessel, and J. Kurths, “Firefly courtship as the basis of the synchronization-response principle,” Europhys. Lett., **94**, 60007 (2011).
- ¹⁶G. M. Ramírez-Ávila, J.-L. Deneubourg, and J. Kurths, “Fireflies: A Paradigm in Synchronization,” in *Chaotic, Fractional, and Complex Dynamics: New Insights and Perspectives.*, edited by M. Edelman, E. Macau, and M. Sanjuan (Springer, Cham, 2018), pp. 35–64.
- ¹⁷Z. Néda, E. Regan, T. Vicsek, and A. Barabasi, “Physics of the rhythmic applause,” Phys. Rev. E. **61**, 6987–6992 (2000).
- ¹⁸S. J. Aton, and E. D. Herzog, “Come together, right...now: Synchronization of rhythms in a mammalian circadian clock,” Neuron. **48**, 531–534 (2005).
- ¹⁹J. Buck, and E. Buck, “Mechanism of rhythmic synchronous flashing of fireflies,” Science, **159**, 1319–1327 (1968).
- ²⁰R. E. Mirollo, and S. H. Strogatz, “Synchronization of pulse-coupled biological oscillators,” SIAM J. Appl. Math., **50**, 1645–1662 (1990).
- ²¹M. Santillán, “Periodic forcing of a 555-IC based electronic oscillator in the strong coupling limit,” Int. J. Bifurcat. Chaos **26**, 1630007 (2016).
- ²²N. Rubido, C. Cabeza, A. C. Martí, and G. M. Ramírez-Ávila “Experimental results on synchronization times and stable states in locally coupled light-controlled oscillators,” Phil. Trans. R. Soc. A, **367**, 3267–3280 (2009).
- ²³G. M. Ramírez-Ávila, J. L. Guisset, and J. L. Deneubourg, “Synchronization in light-controlled oscillators,” Physica D, **182**, 254–273 (2003).
- ²⁴N. Rubido, C. Cabeza, S. Kahan, G. M. Ramírez-Ávila, and A. C. Martí, “Synchronization regions of two pulse-coupled electronic piecewise linear oscillators,” Eur. Phys. J. D., **62**, 51–56 (2011).
- ²⁵M. Abel, S. Bergweiler, and R. Gerhard-Mulhaupt, “Synchronization of organ pipes: Experimental observation and modeling,” J. Acoust. Soc. Am., **119**, 2467–2475 (2006).
- ²⁶K. Okamoto, A. Kijima, Y. Umeno, and H. Shima, “Synchronization in flickering of three coupled candle flames,” Sci. Rep. **6**, 36145, (2016).
- ²⁷A. Koseska, E. Volkov, and J. Kurths, “Oscillation quenching mechanisms: Amplitude vs. oscil-

lation death,” *Phys. Rep.* **531**, 173–199 (2013).

²⁸A. Pikovsky, M. Rosenblum, and J. Kurths, *Synchronization: A Universal Concept in Nonlinear Sciences*, (Cambridge University Press, Cambridge, 2001).

²⁹T. Banerjee, and D. Ghosh, “Experimental observation of a transition from amplitude to oscillation death in coupled oscillators,” *Phys. Rev. E* **89**, 062902 (2014).